

# Analyst

Accepted Manuscript



This is an *Accepted Manuscript*, which has been through the Royal Society of Chemistry peer review process and has been accepted for publication.

*Accepted Manuscripts* are published online shortly after acceptance, before technical editing, formatting and proof reading. Using this free service, authors can make their results available to the community, in citable form, before we publish the edited article. We will replace this *Accepted Manuscript* with the edited and formatted *Advance Article* as soon as it is available.

You can find more information about *Accepted Manuscripts* in the [Information for Authors](#).

Please note that technical editing may introduce minor changes to the text and/or graphics, which may alter content. The journal's standard [Terms & Conditions](#) and the [Ethical guidelines](#) still apply. In no event shall the Royal Society of Chemistry be held responsible for any errors or omissions in this *Accepted Manuscript* or any consequences arising from the use of any information it contains.

## ARTICLE

# Transmission versus transflection mode in FTIR analysis of blood plasma: is the EFSW effect the only reason of the observed spectral distortions?

Cite this: DOI: 10.1039/x0xx00000x

Received 00th January 2012,  
Accepted 00th January 2012

DOI: 10.1039/x0xx00000x

www.rsc.org/

Emilia Staniszewska-Slezak,<sup>a,b</sup> Anna Rygula,<sup>b</sup> Kamilla Malek<sup>a,b\*</sup> and Malgorzata Baranska<sup>a,b</sup>

Fourier transform infrared (FTIR) microspectroscopy is assessed in terms of the two techniques, i.e. transmission and transflection, as a method for the rapid measurements of blood plasma. Apart from the expected effect of the electric field standing wave (EFSW), we also noticed that second derivative IR spectra recorded in transflection mode exhibit a significant shift of amide I band (up to 1667 cm<sup>-1</sup>) in comparison to the one recorded in transmission (1658 cm<sup>-1</sup>). This has not been reported so far in studies on the EFSW distortion of IR spectra of biological material. The thinner the sample is deposited on the low-*e* microscope slide, the lower position of the amide I band is found in FTIR spectra, suggesting various composition of plasma after stratification or some changes in protein secondary conformations due to chemical and/or physical effects. There are potentially several phenomena which can occur at the surface of both IR substrates affecting the protein profile and among them we considered: 1/ changes in optical properties (refractive index), 2/ variation in water content in the sample and 3/ segregation of plasma components. All these hypotheses are discussed here, with the help of Atomic Force Microscopy (AFM).

## Introduction

A wide analytical application of FTIR microspectroscopy in studies on tissue sections, cell cultures or any biological material has been shown in numerous reports<sup>1-5</sup>. The choice of the biological material for diagnostic purpose is dictated by the presence of a proper marker for a disease, and to date plasma and serum are preferable in medical diagnostics due to their least invasive way of sample collection from patients. On the other hand, the use of FTIR spectroscopy for such purposes requires a reliable and rapid approach. A careful examination of factors affecting spectral FTIR profiles, standardization of sample preparation and spectral measurements are still necessary<sup>6-10</sup>. For instance, Ollesch and co-workers have recently reported a detail review on FTIR microspectroscopy of serum and plasma showing advantages of the measurement of undiluted and dried plasma samples in transmission mode for the diagnosis of urinary bladder cancer<sup>6</sup>. Similar results have been shown in studies on ovarian cancer using ATR FTIR spectra of plasma and serum<sup>11</sup>.

In our approach we use imaging technique of FTIR spectroscopy to analyse spectral profile of plasma. This provides a rapid method of data collection with the use of a commercially available FTIR microscope, since a few thousands of spectra within a few minutes are recorded from a minimal volume of an air-dried sample (0.5 – 1 µL) to remove water obscuring infrared spectra. To maximize the sensitivity of this approach, the drop coating deposition substrates must be carefully chosen. As it is well known, inorganic crystals like CaF<sub>2</sub> windows and metal microscope slides

have been commonly used for transmission and transflection FTIR measurements, respectively. We chose both techniques and CaF<sub>2</sub> and Ag/SnO<sub>2</sub>-coated microscope slides, respectively, for our studies on FTIR profile of plasma. It has been demonstrated that the electric field standing wave (EFSW) can lead to significant distortion of transflection FTIR spectra of biological samples like tissues and cells<sup>12-14</sup>. The major issue of EFSW corresponds to non-linear response of absorbance along with the increase of sample thickness, consequently leading to alternation of band ratios. To our best knowledge, no other spectral distortions associated with the electric field standing wave effect have been reported to date. An impact of this effect on an analysis of FTIR spectra can be reduced by calculation of second derivative spectra<sup>13</sup>. Moreover, Wrobel et al. have shown in simulation of experimental variability that distortion of infrared spectra by the EFSW is almost completely averaged out for inhomogeneous samples of sufficient thickness (ca. 5 µm) while changes in intensity ratios become more significant for samples of thickness below 2 µm<sup>15</sup>.

The aim of our work is a comparison of IR optical substrates dedicated for measurements of biofilms by using both the most popular techniques, i.e. transmission and transflection, and to check if the EFSW is the only reason of the observed spectral distortions. For that we performed an examination of topography and spectral features of plasma deposits placed on two common slides, i.e. the CaF<sub>2</sub> window and the MirrIR (Ag/SnO<sub>2</sub>) slide. Each of the IR substrates represents different chemical, surface and optical properties, and apart from a potential distortion of spectra features due to the EFSW, questions can arise whether both types of FTIR

spectra of the same plasma sample provide similar spectral profile of this biological material. Observed spectral differences are discussed along with topography and adhesion measurements using Atomic Force Microscopy (AFM).

## Experimental

### Sample preparation

All animal experiments were performed in accordance with institutional guidelines and were approved by the Animal Care and Ethics Committee of the Jagiellonian University. Blood samples were collected from three healthy mice C57 BL/6J with the use of 10 u. nadroparin per 1 ml of blood as an anti-clotting agent. Blood was centrifuged at 1 000g for 10 min, and then plasma were immediately separated. Time between blood collection and centrifugation was approximately 10 min. Next 1  $\mu$ l and 0.5  $\mu$ l of each samples were manually spotted onto low-*e* microscope slides (MirrIR, Kevley Technologies®) and CaF<sub>2</sub> windows, respectively, and left to dry in a temperature-controlled laboratory (24 °C). Both IR substrates unused before the experiment were cleaned in an autoclave and wiped off with ethanol before deposition of plasma samples. The drying process took approximately 3 min giving deposits with ca. 5 mm in diameter on both substrates. The volume of plasma was adjusted to provide FTIR spectra with absorbance below 1.2. To investigate if there is an effect of water content on FTIR profile of plasma measured by using the transflection technique, the low-*e* microscope slide was heated to temperature of 45 °C, and after that the plasma drop was placed on the slide. The manufacturer of the MirrIR slides (Kevley Technologies, Ohio) provides information that the slides are stable till 400 °C, so chemical/physical changes on the surface of the slides should be excluded. For this experiment, we used plasma of two mice.

### FTIR imaging and data processing

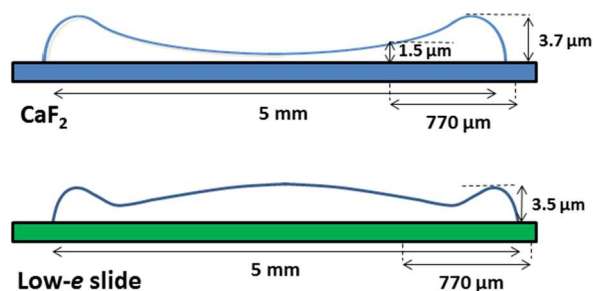
Liquid nitrogen cooled MCT FPA (Mercury Cadmium Telluride Focal Plane Array) detector comprising 4096 pixels arranged in a 64×64 grid format was used to measure FTIR images with a Agilent 670-IR spectrometer and 620-IR microscope operating in rapid scan mode. Transflection and transmission measurements were recorded with a 15× Cassegrain objective collecting 64 scans from a plasma sample deposited on a low-*e* microscope slide and a CaF<sub>2</sub> window, respectively. Background measurements were acquired on blank substrates with 128 scans per pixel. All spectra were collected in the range of 3800 – 900 cm<sup>-1</sup> with a spectral resolution of 8 cm<sup>-1</sup>. The imaging area measured using this accessory and this FPA detector was ca. 350×350  $\mu$ m<sup>2</sup> with each pixel sampling from an area of 5.5×5.5  $\mu$ m<sup>2</sup>. Recording 4096 spectra took 3 min. For one of the plasma samples air-dried at room temperature on both slides, the same imaged area was investigated next by using the AFM techniques.

FTIR spectra embedded in each spectral image were first quality-screened and then extracted using a CytoSpec v. 1.4.03 software<sup>16</sup>. The quality test for sample thickness was performed according to the absorbance over the „fingerprint region” (900-1750 cm<sup>-1</sup>) to remove spectra with the maximum absorbance less than 0.4 or greater than 1.2. Then second derivative spectra were calculated using a Savitzky- Golay algorithm (9 points of smoothing). Cluster maps were constructed by using Unsupervised Hierarchical Cluster Analysis (UHCA) in the spectral regions of 900 – 1800 and 2800 – 3600 cm<sup>-1</sup>. For UHCA imaging, a Ward's algorithm was used, while

spectral distances were computed as D-values. An analysis of cluster maps indicated that 5 classes represent a general trend of variation observed in transflection FTIR spectra. For comparison, 3- and 7-class UHCA analysis is shown in Figure S1 (in Electronic Supplementary Material). The same parameters were employed in UHCA analysis of transmission chemical images. For each cluster map, the mean spectrum was extracted while integral intensities for selected bands were calculated by using a OPUS 7.0 software. A straight line was drawn between the peaks of the two frequency limits defined. The area above and below this line was integrated for raw and second derivative FTIR spectra, respectively.

### Atomic Force Microscopy (AFM) measurements

The AFM measurements were performed with a WITec alpha 300 system in PFM modes using Force Modulation probes ( $k=2.8$  N/m, WITec). The area of 770×20  $\mu$ m<sup>2</sup> was scanned for each sample in both AFM modes, by composed of five smaller images. The resolution of images was 512×64 pixels for an area of 150×20  $\mu$ m<sup>2</sup>. 20  $\mu$ m of each small image was overlapped with the next one. The PFM mode is working in intermediate contact mode but with non-resonance frequency, so as a result of measurement, apart from the topography, the mechanical surface properties like adhesion and stiffness are acquired. It has to be said, that the software version which was used here, does not have any option of the AFM system calibration and recalculation of results to proper units. Therefore, we present the adhesion parameter in relative values (volts) which are raw data delivered by the software and they are proportional to adhesion force.



**Scheme 1.** A schematic draw showing shapes of plasma deposits on the CaF<sub>2</sub> window (upper) and the low-*e* microscope slide (down).

## Results and discussion

### Topography of the plasma deposits

As seen from Figures 1A and 2A, the dried spots of mice plasma placed onto both substrates represent slightly different morphologies. A schematic cross section of both deposits is depicted in Scheme 1. Topography of both samples from their edges within the distance of 770  $\mu$ m were measured using AFM technique whereas the overall shape were concluded from changes in absorbance of the amide I band in IR images (Fig. S2 in Electronic Supplementary Material). A typical “coffee-ring” was formed for plasma placed on the CaF<sub>2</sub> slide due to pre-concentration of the sample upon evaporation of the material on the surface, *cf.* Fig. 1A, Scheme 1. The AFM topography of this sample shows changes in the thickness of the deposit from 1.5 to 4.0  $\mu$ m through the distance of 770  $\mu$ m from the edge of the sample (Fig. 1B).

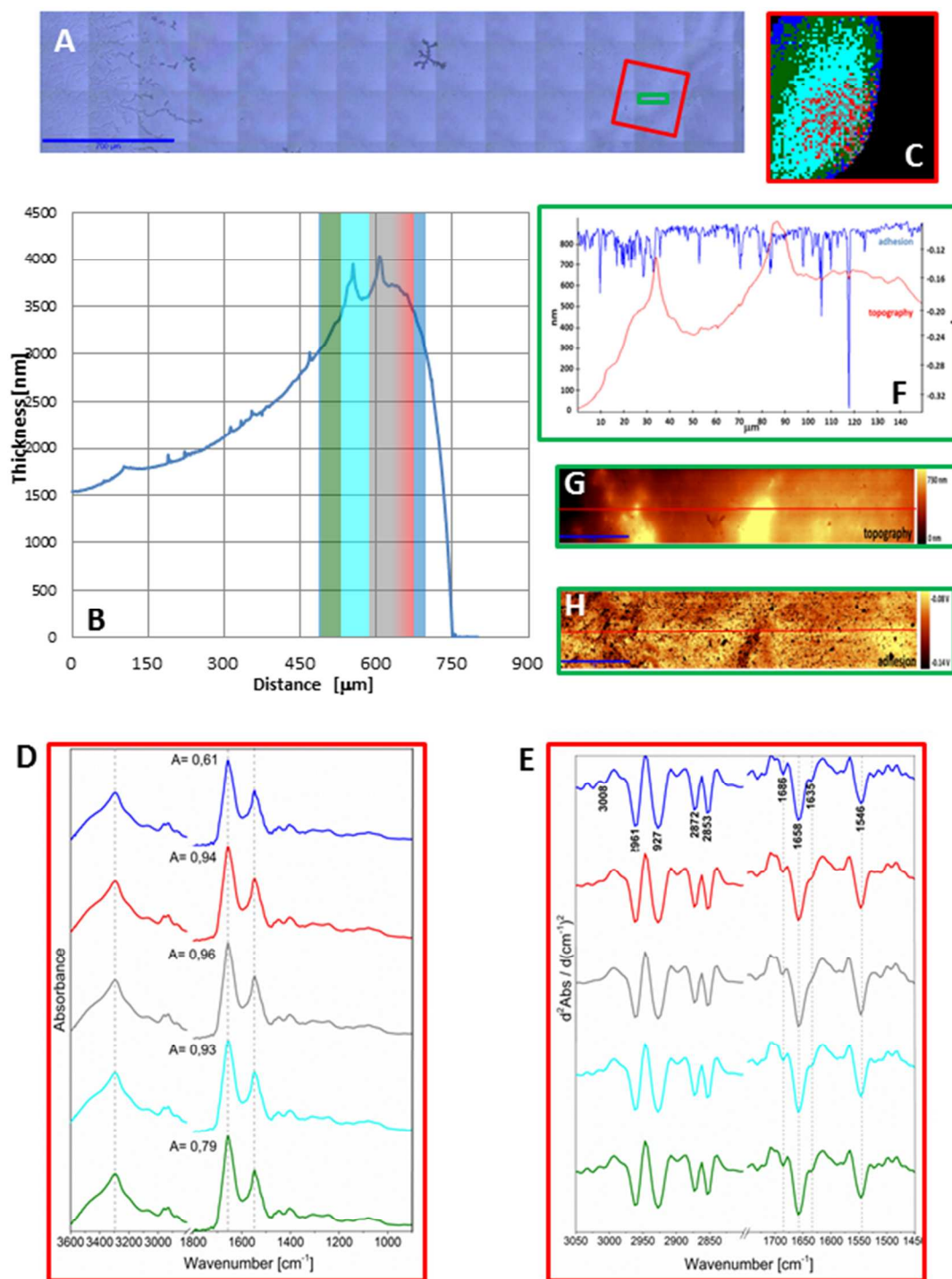


**Figure. 1** (A) Photomicrography of the plasma sample deposited on the CaF<sub>2</sub> window (animal 1). The orange and green rectangles, respectively, indicate the area selected for FTIR imaging in transmission mode (350×350 μm<sup>2</sup>) and an AFM image corresponding to an area of UHCA analysis (20×150 μm<sup>2</sup>); (B) a 770 μm AFM profile for the plasma sample, the colours within the graph correspond to classes of the UHCA analysis in (C); (C) 5-cluster map constructed using UHCA; (D) mean FTIR spectra extracted from the cluster map in (C), the colours of the spectra correspond to the colours of the clusters; (E) the second derivative spectra from (D), the region of 2800 – 3050 cm<sup>-1</sup> is enlarged 8×; (F) the cross section of topography and adhesion along the red line labelled in (G) and (H), respectively; (G) AFM topography and (H) adhesion images of the green area from (A).



## ARTICLE

A few reports have shown that such a deposit of biological material results in a flow of solute material from the centre of the drop to its perimeter<sup>6,17-19</sup>.

In turn, a slightly different cross-section of plasma is found for the sample placed on the low-*e* microscope slide (Scheme 1, Figs. 2B and S2 in ESI). Here, the deposit becomes thicker going from the periphery to the centre, then forming a thinner ring and again it becomes almost thick as in the periphery of the sample. In addition, the white light images of both samples show the presence of fern-like patterns in the centre of the samples (Figs. 1A and 2A). This is an effect of crystallisation of electrolytes such as NaCl, bicarbonates and urea<sup>17</sup>. More patterns are formed in the centre of the plasma drop deposited on the low-*e* slide than on the CaF<sub>2</sub> substrate. The formation of similar fern-like patterns has been observed in deposits of tears and human serum investigated by means of Raman spectroscopy<sup>17,18</sup>.

### IR features of the plasma deposits

Figures 1C and 2C depict 5-class cluster maps of plasma (animal 1) constructed with the use of unsupervised hierarchical cluster analysis (UHCA) while Figures 1 D,E and 2 D,E show mean FTIR spectra with their second derivatives recorded in the transmission and transfection techniques, respectively.

At first glance, mean FTIR spectra of plasma recorded in the transmission and reflection geometry are found to be similar, showing the same general spectral profile, including the presence of normal modes of the common biological macromolecules (proteins, lipids, etc.), *cf.* Figs. 1D and 2D. Total absorbance of IR spectra recorded in the transmission technique changes almost linearly along with the thickness of the samples as depicted by absorbance of the amide I band (see Fig. 1B,D) in contrast to transfection IR spectra (see Fig. 2B,D). Next, we compared the intensity ratio for bands of the methyl groups observed at 2962 and 1446 cm<sup>-1</sup> [ $v_{as}(\text{CH}_3)/\delta(\text{CH}_3)$ ] to identify spectral variation resulting from the electric field standing wave effect, see Table 1. As expected, this ratio negligibly changes in spectra collected in the transmission geometry whereas it varies from 0.8 to 1.8 for transfection spectra. For the latter, the ratio is constant for the 0.12 - 0.50  $\mu\text{m}$  thickness of plasma (ca. 0.8, green and cyan classes, see Fig. 2C and Table 1), and then it considerably rises for the other classes with the thickness in the range of 0.5 - 1.5  $\mu\text{m}$ , indicating a strong effect of EFSW. According to Wrobel and co-workers, a strong contribution of the EFSW is expected for samples of the thickness below ca. 5  $\mu\text{m}$ <sup>15</sup>.

Apart from this effect, we also noticed that second derivative IR spectra recorded in the transfection mode exhibit a significant shift of amide I and II bands in comparison to the ones recorded in transmission. This has not been reported so far in studies on the EFSW distortion of IR spectra of biological material<sup>12-15</sup>. The observed spectral differences in the amide I/II region are depicted in Figure 2E and summarized in Table 1. All transmission IR spectra of the same plasma sample show the presence of both amide bands at 1658 and 1547 cm<sup>-1</sup> (*cf.* Fig. 1E, Table 1). The same observation was found in FTIR

spectra of plasma of two other animals indicating that spectral profile does not change between individuals, see Figures S3 and S4, in ESI. For the transfection geometry, the position of the amide I band shifts from 1667 cm<sup>-1</sup> for the thickest class (the grey cluster) to 1651 cm<sup>-1</sup> for the thinnest investigated fragment (the green cluster, in Fig. 2 B,E, so in comparison to the transmission measurement (1658 cm<sup>-1</sup>) it is shifted down to 7 cm<sup>-1</sup> and up to 9 cm<sup>-1</sup>. A graph in Figure 3A illustrates that the relationship between the position of the amide I band and the sample thickness is proportional in transfection measurements. It means that the thinner the sample is deposited on the low-*e* microscope slide, the lower position of the amide I band is found in FTIR spectra. This observation suggests changes in composition of plasma after stratification or segregation of plasma proteins in contact with the low-*e* microscope slide or physical effects. There are probably several phenomena which can occur at the surface of both IR substrates affecting the spectral profile and among them we considered: 1/ changes in optical properties/reflective index, 2/ variation in content of water, and 3/ segregation of proteins/biomolecules due to their flow on the IR substrate. Let's discuss all these hypotheses.

**Table 1.** The comparison between the selected spectral features of mean FTIR spectra (from UHCA analysis depicted in Figs. 1C and 2C) and topography of the plasma deposits on the CaF<sub>2</sub> and low-*e* slides. For transmission, the range of values is only given due to good reproducibility of spectra among UHCA classes.

Class	Thickness of the plasma deposit [ $\mu\text{m}$ ]	$v_{as}(\text{CH}_3)/\delta(\text{CH}_3)$ ratio	Position of amide I [ $\text{cm}^{-1}$ ]	amide I/ amide II ratio	amide I/ amide II ratio
<b>Transfection mode</b>					
Green	0.12 – 0.32	0.85	1651	3.86	1.85
Cyan	0.32 – 0.49	0.83	1659	5.39	1.95
Red	0.49 – 1.01	1.47	1663	6.09	3.27
Blue	1.01 – 1.11	1.31	1665	9.56	3.60
Grey	1.11 – 1.50	1.82	1667	8.78	2.78
Average values from all spectra		0.48	1658	7.25	2.06
<b>Transmission mode</b>					
	3.00 – 3.75	0.29-0.32	1658	6.07-6.29	2.07-2.15

1/ One can assume that the observed changes in position of amide I and II bands of plasma deposited on the MirrIR window rely on physical phenomena. Since we collected IR images close to the edge of the deposit (see Figs. 1 and 2 A,B), our findings can result from anomalous dispersion of the refractive index. Romeo and Diem showed strongly distorted infrared spectra recorded in transfection mode at the edges of the 5  $\mu\text{m}$  tissue sections.<sup>20</sup> These artifacts result in shifting bands, especially amide I, toward lower wavenumbers up to 30 cm<sup>-1</sup> and distortion of amide I/amide II ratio. They also reported that this effect can appear in transmission spectra.<sup>20</sup>

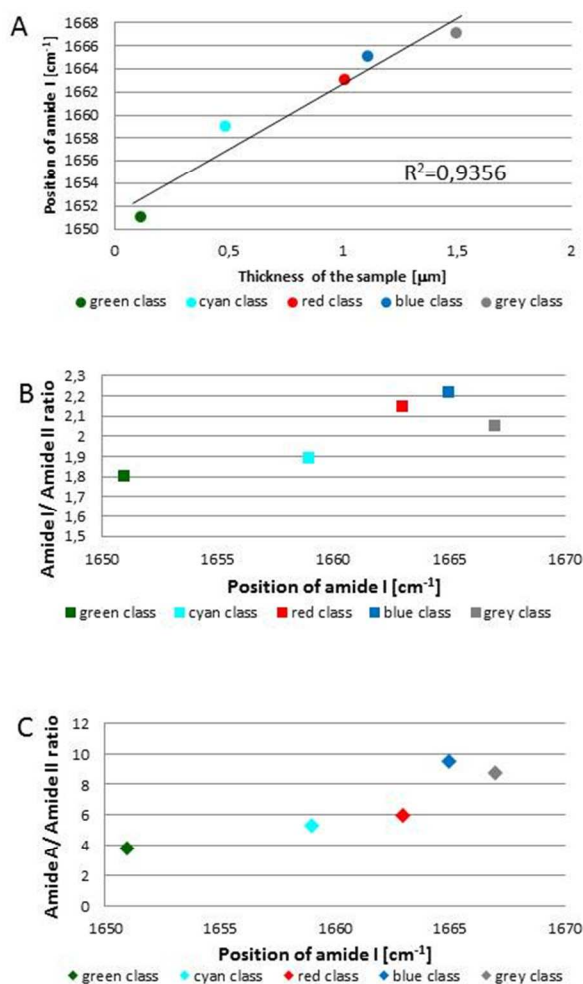


**Figure 3.** Variation of the position of the amide I band as a function of the sample thickness with fitting to a linear function for each class of UHCA analysis in transfection FTIR spectra (A), variation in the amide I / amide II band ratio (B) and amide A / amide II band ratio (C) as a function of the position of the amide I band. The colours on the graphs correspond to the colours of UHCA classes in Fig. 2C.

Figure S5 (in Electronic Supplementary Material) displays all raw spectra extracted from the thinnest and thickest classes of UHCA for both geometries. This comparison clearly shows that all spectra are not distorted in a manner illustrated in<sup>20</sup>. None of them exhibits a scattering background. Transmission spectra are virtually identical with changes in total absorbance (Fig. S5 A,B) as discussed above while transfection spectra mainly differ in relative intensity between the fingerprint and wavenumber regions indicating the presence of EFSW (Fig. S5 C,D).

The other explanation of the observed shift of the amide bands can rely on differences in refractive indices of both IR windows. Wehbe et al. have also observed differences in the amide I position in average FTIR spectra collected from cells grown on the crystal inorganic salts<sup>14</sup>. The maximum of the amide I band was shifted from 1656.0 to 1654.5 cm<sup>-1</sup> on ZnS and CaF<sub>2</sub>, respectively. This was explained by the occurrence of optical artifacts associated with a lower refractive index of CaF<sub>2</sub> (1.4) in comparison to ZnS (2.25). In our work, we

observe the 1658 cm<sup>-1</sup> band recorded on the CaF<sub>2</sub> substrate and the bands in range of 1651- 1667 cm<sup>-1</sup> for plasma on the MirrIR slide, while the refractive indexes of the CaF<sub>2</sub> and MirrIR slides are 1.4<sup>14</sup> and 2.0<sup>24</sup>, respectively.<sup>14,24</sup> In addition, when we compare mean transmission and transfection spectra from the whole IR images like in the work of Wehbe<sup>14</sup> both amide I bands are observed at the same position and bands ratios of the average transfection spectrum are very similar to those calculated for the average transmission spectrum, see Table 1. One can also consider the contribution of other effects such as Mie scattering or Fresnel reflection to the observed distortion of transfection FTIR spectra. However, the contribution of Mie scattering would suggest that the plasma deposit on the low-*e* microscope slide consists of particles of the size similar to the wavelength that scatter the infrared light. This effect is rather excluded hence FTIR spectra of both deposits should exhibit similar distortions. In turn, Mitlin and Leung have reported changes in intensity, shape and position of the OH stretching mode of ice films deposited on a metal surface in FTIR reflection-absorption spectra as a function of the film thickness.<sup>25</sup> They have noted that the OH dangling bonds located on the external surface of the film and the formation of different ice phases upon increasing film thickness strongly affect reflection coefficients for parallel- and perpendicular-polarized IR light. However, such changes of spectra could be also attributed to the differences in the structures of the water network.<sup>25</sup> That suggests that a complex optical phenomenon or/and artefacts must be considered to understand fully the observed variation in the amide I/II positions within an area of ca. 350×350 μm<sup>2</sup>. If it is this case, it is also worth-mentioning here that no other bands are shifted and the amide bands show the highest intensity in IR spectrum, suggesting that artefacts in the transfection spectra of plasma may rather result from a potential optical distortion of high-intensity bands than from changes in the protein structure.

2/ A close examination of the secondary derivative IR spectra in Figs. 1E and 2E shows the presence of a typical amide I band at ca. 1658 cm<sup>-1</sup> ( $\alpha$ -helices) accompanied by shoulders at ca. 1680-1686 and 1632-1639 cm<sup>-1</sup>. A band at ca. 1680 cm<sup>-1</sup> is attributed to antiparallel  $\beta$  sheet conformations of proteins whereas the 1635 cm<sup>-1</sup> band can be assigned either to a  $\beta$ -sheet structure or to the bending vibration of water molecules. The intensity of the latter does not change in the transmission IR spectra (Fig. 1E) whereas it increases significantly in the thick layers of plasma deposited on the low-*e* slide (blue and grey traces in Fig. 2E). We also noticed an increase of intensity of an amide A band and a band at 1681 cm<sup>-1</sup> in FTIR spectra of these classes (Fig. 2D,E). Next, we calculated ratios of integral intensities for the amide A and II bands and the amide I and II bands to examine the presence of water, see Table 1, Fig. 3B,C. For plasma deposited on the MirrIR slide with the thickness up to 0.5 μm (green and cyan classes), both ratios are similar and then they increase significantly for the red and blue classes. Interestingly these values become lower for the thickness above 1.1 μm (the grey class) for that we observe the highest intensity of the 1634 cm<sup>-1</sup> band. Large variation in the amide A/amide I ratio may rather result from the EFSW since Wrobel et al. showed that a strong effect of the EFSW is observed for the sample thickness below 2 μm, especially when we compare intensities of bands from the high-wavenumber and fingerprint regions<sup>15</sup>. In turn, intensities of bands closely appearing in the IR spectrum, i.e. amide I and II, should not be strongly affected by the EFSW. In our case, the amide I/amide II ratio changes within 1.85 – 3.60 in the mean spectra in the transfection geometry whereas it is ca. 2.0 in the transmission IR spectra (typical for a biological sample). This fact shows that the

contribution of water vibrations to the amide I band should be considered. Firstly, we examined if time of drying the sample of plasma affects spectral profile of the transfection FTIR spectra. Figure S6 in Electronic Supplementary Information shows FTIR spectra of plasma recorded after 1 h and 1 month from depositing the sample on the low-*e* microscope slide. Since they are similar to those displayed in Fig. 2E spectral changes are observed, we assumed that the overall spectral profile of plasma is not affected by slow evaporation of water from plasma. Next, to exclude or confirm a

possible contribution of water to changes in protein structures during drying of plasma, we heated a low-*e* microscope slide to 45 °C before depositing the plasma sample to accelerate evaporation of water from plasma and to assign properly the 1635 cm<sup>-1</sup> band. A cluster map and FTIR spectra depicted in Figure 4 clearly shows that a shift of the amide I and II bands remains but a band at ca. 1635 cm<sup>-1</sup> almost disappears.

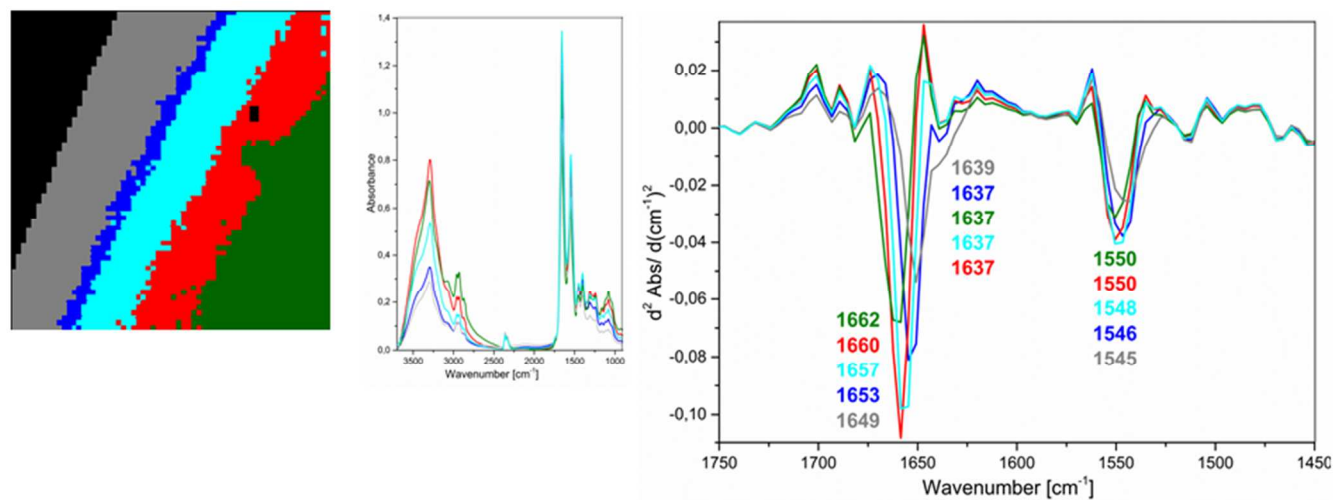


**Figure 4.** UHCA analysis for plasma deposited on the low-*e* slide heated to 45 °C: 5-class cluster map along with mean spectra and their second derivatives corresponding to each class.

Therefore, we concluded that this band of high intensity in the grey class in Fig. 2 should be rather assigned to the bending vibrations of water molecules than to an amide I band of  $\beta$ -pleated structure of proteins. This observation also indicates that the spectral variation in the amide region of the transfection IR spectra is not associated with drying rate of plasma but a content of water.

To examine this issue closely, we recorded FTIR images across the plasma deposit placed on both substrates. Figure S7 (in Electronic Supplementary Material) shows UHCA analysis for the transmission geometry. Mean second derivative FTIR spectra are similar to those displayed in Fig. 1E confirming that the amide I/II spectral region recorded using this technique is “homogenous” across the whole deposit. In general, slight change in the intensity of a shoulder at ca. 1635 cm<sup>-1</sup> indicates variation of content of water in particular in the centre of the sample where fern-like patterns are present. Figure 5 illustrates a detailed UHCA analysis and second derivative spectra of the plasma deposit placed on the low-*e* microscope slide. A cluster map for the whole deposit clearly shows that FTIR profile of plasma deposited on this IR substrate exhibits a stripe-like pattern, see Fig. 5 A. Its mean FTIR spectra indicates that

spectra from the edge of the deposit represent the IR features typical for the transmission FTIR spectra (red trace in Fig. 5C) whereas spectra from the other classes exhibit the presence of the amide I band at 1664 cm<sup>-1</sup> along with increasing intensity of two shoulders at 1685 and 1635 cm<sup>-1</sup> going from the edge to the centre of the sample. Since we assigned the 1635 cm<sup>-1</sup> to water and the two other bands (1664 and 1685 cm<sup>-1</sup>) are clearly associated with the amide I vibrations, it is expected that increasing water content in the sample changes a H-bonding 3D-network resulting in modifications of protein structure. A contribution of other plasma components like electrolytes is also expected. We selected some smaller regions of interest to show changes in FTIR profile in detail, *c.f.* Fig. 5B. Second derivative spectra in the amide I/II region from ROI 1 show variation in the position of both amide bands as previously discussed but without a contribution of water (Fig. 5D) whereas FTIR spectra from ROI 2 and 3 exhibit spectral features typical for a high content of water. We roughly estimated that the most pronounced changes in wavenumbers of the amide bands appear within ca. 500  $\mu$ m from the edge of the deposit.

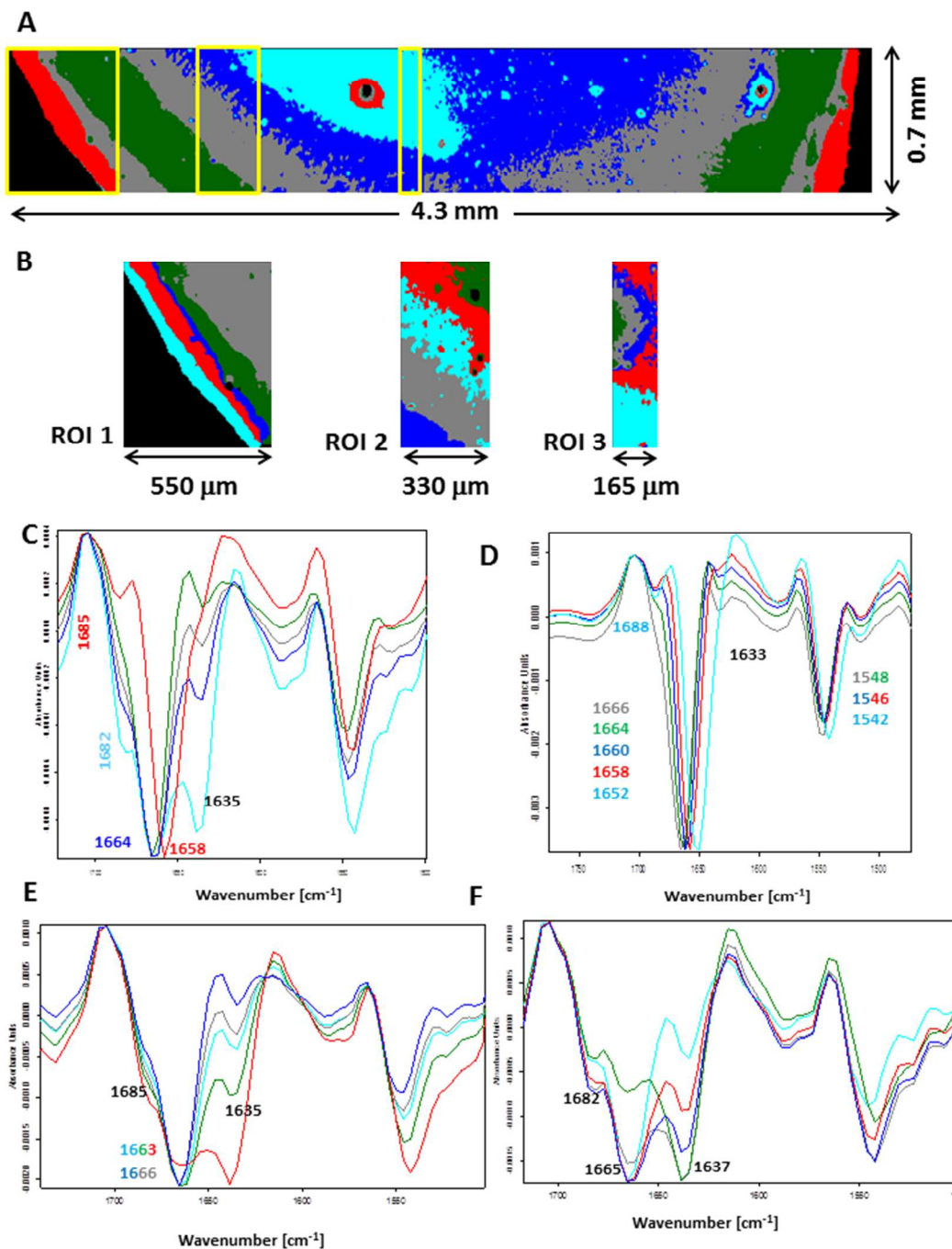


**Figure 5.** (A) 5-class cluster map for the plasma sample deposited on the low-e microscope slide; yellow rectangles denote selected regions of interest (ROI); (B) 5-class cluster maps for each ROI labelled by yellow rectangles in (A); (C) mean second derivative FTIR spectra in the region of 1700 – 1500 cm<sup>-1</sup> for the cluster map in (A); (D) mean second derivative FTIR spectra in the region of 1700 – 1500 cm<sup>-1</sup> for the cluster map of ROI 1 in (B); (E) mean second derivative FTIR spectra in the region of 1700 – 1500 cm<sup>-1</sup> for the cluster map of ROI 2 in (B); (F) mean second derivative FTIR spectra in the region of 1700 – 1500 cm<sup>-1</sup> for the cluster map of ROI 3 in (B). The colours of the spectra correspond to the colours of the clusters.

## ARTICLE

3/ Segregation of proteins due to flow of the bodily fluids during evaporation is a well-documented fact easily observed in IR and Raman studies<sup>17,19,22,23</sup>. However, this corresponds to differences in the chemical/protein composition and content in the centre of the fluid deposit and its perimeter. Actually, the highest concentration of proteins is found at the edge of a drop of the bodily fluid if the “coffee ring” is formed. There are no reports to our best knowledge that such separation process also occurs within the periphery of the coffee ring and this is confirmed by our transmission IR spectra. During deposition of the plasma sample on both IR substrates, we noticed that plasma can be easily spread on the surface of the low-*e* microscope slide than on the CaF<sub>2</sub> window. This means that cohesive forces are weaker than adhesive forces between plasma and the reflective coating of the low-*e* slide. It is also consistent with hydrophobic properties of the CaF<sub>2</sub> surface<sup>14</sup>. We used atomic force microscope (AFM) to investigate if there are differences in adhesion forces of the windows and plasma. We also compared the adhesion parameters of the clean substrates. For the latter, AFM measurements were performed under identical instrumental so we can confidently compare values of adhesion forces that are -0.082 and -0.113 V for the CaF<sub>2</sub> and low-*e* windows, respectively. This confirms that the latter exhibits stronger adhesion features than the CaF<sub>2</sub> window. Figures 1,2 F-H show how adhesion changes within the investigated area on the surface of the deposited plasma. First of all, this reveals that regardless of the sample thickness, adhesion forces do not change for plasma deposited on the CaF<sub>2</sub> window whereas they regularly oscillate within the plasma ring placed on the MirrIR slide. This suggests that physical/chemical properties of the dried plasma deposited on both substrates are different but not due to segregation of proteins and/or other biocomponents since adhesion forces do not vary between the UHCA classes. Taking into account our adhesion measurements as well as the fact that there are no significant differences in adhesion forces of the blood plasma proteins such as albumin, fibrinogen and immunoglobulin on hydrophilic and hydrophilic surfaces<sup>21</sup> we assumed that the segregation of proteins on the low-*e* microscope slide is not reflected by transflection IR spectra.

## Conclusions

Comparing the results for the plasma measured by using two infrared imaging modes, transmission and transflection, one can see significant differences between them. Spectra collected in transmission mode show the same positions of the amides bands and the ratio of their intensities regardless of the thickness of the measured sample. Notwithstanding measurements of plasma in transflection mode are disturbed and strongly depend on the thickness of the biofilm sample. Some spectral disturbances can be explained by the expected electric field standing wave effect, but the shift of amide I (1651-1667 cm<sup>-1</sup>) band in comparison to the one recorded in transmission (1658 cm<sup>-1</sup>) has not been reported until now. It is clear for everyone that IR light passes through the sample in a different manner in both techniques and this can be a primary reason for the observed variations in spectral features. However, if we compare transflection FTIR of plasma with thickness of 1.5 μm with transmission ones for the sample with

thickness of ca. 3 μm, we still observe a 9 cm<sup>-1</sup> difference in the wavenumber of the amide I bands, see the grey and green classes in Figs. 1 and 2, respectively. Our discussion showed that two effects can contribute to our observation, namely variation in content of water and optical artefacts. However, in the case of the latter we excluded typical light dispersion and Mie scattering observed previously in chemical images of tissues. Water molecules strongly change FTIR features of plasma proteins in the centre of the deposit placed on the MirrIR slide on contrary to the CaF<sub>2</sub> window whereas optical phenomena are very likely responsible for changes observed at the edge of the deposit. In addition, the discussed differences in the surface features of both plasma deposits and variation in the water content in plasma placed on the MirrIR slide may indicate modulation of reflected and refracted infrared light like in the Fresnel phenomenon that leads to the observed spectral differences between transflection and transmission geometry.

To sum up, it seems that the reported so far EFSW effect is not the only reason of the spectral distortions observed in the measurements in transflection mode, in particular for a liquid biomaterial, suggesting that further investigations on the use of this FTIR technique should be continued. Several efforts must be undertaken to study to what extent the transflection geometry can be employed for measurements of chemically heterogeneous fluids, especially that the other similar studies showed that relatively flat and properly thick tissue cross-sections can be still examined by means of this FTIR mode for diagnostic purpose when chemical changes due to pathology are pronounced.

## Acknowledgements

This work was supported by National Center of Science (DEC-2013/08/A/ST4/00308) and by the European Union from the resources of the European Regional Development Fund under the Innovative Economy Programme (grant coordinated by JCET-UJ, No POIG.01.01.02-00-069/09).

## Notes

<sup>a</sup> Faculty of Chemistry, Jagiellonian University, Ingardena 3, 30-060 Krakow, Poland

<sup>b</sup> Jagiellonian Centre for Experimental Therapeutics (JCET), Jagiellonian University Bobrzynskiego 14, 30-348 Krakow, Poland

\*CORRESPONDING AUTHOR: K. Malek, e-mail:

malek@chemia.uj.edu.pl, phone/fax: +48 12 663 2064/+48 12 634 0515

Electronic Supplementary Information (ESI) available:

**Figure S1.** 3- and 7-class UHCA analysis of FTIR images for the transflection mode. Second derivative spectra represent mean spectra of each class. Colors of spectra correspond to the colors in cluster maps; **Figure S2.** Chemical images for the amide I band constructed on raw FTIR spectra from the deposits of plasma placed on a CaF<sub>2</sub> window (A) and a low-*e* microscope

slide (B). **Figure S3.** UHCA analysis for plasma of two other animals (transmission mode): (A) 5-class cluster map along with mean FTIR spectra and their second derivatives corresponding to each class (animal 2); (B) 5-class cluster map along with mean FTIR spectra and their second derivatives corresponding to each class (animal 3); **Figure S4.** UHCA analysis for plasma of two other animals (transfection mode): (A) 5-class cluster map along with mean FTIR spectra and their second derivatives corresponding to each class (animal 2); (B) 5-class cluster map along with mean FTIR spectra and their second derivatives corresponding to each class (animal 3); **Figure S5.** Raw FTIR spectra extracted from UHCA analysis for (A) transmission geometry (blue and magenta classes in Fig. 1C) and (B) transfection geometry (green and grey classes in Fig. 2C); **Figure S6.** 5-class UHCA analysis of plasma after 1-hour (A) and 1-month (B) storing a sample on a low-e microscope slide in a desiccator; **Figure S7.** 5-class UHCA analysis of the whole plasma deposit for FTIR image collected in the transmission mode. Second derivative spectra represent mean spectra of each class. Colors of spectra correspond to the colors in cluster maps.

See DOI: 10.1039/b000000x/

## References

- 1 M. Diem, P.R. Griffiths, J.M. Chalmers (Eds), *Vibrational Spectroscopy for Medical Diagnosis*, Wiley, Chichester, UK, 2008
- 2 K. Malek, B.R. Wood, K.R. Bambery, in: M. Baranska (Ed), *Optical Spectroscopy and Computational Methods in Biology and Medicine*, Springer, 2014, pp. 419-474
- 3 T.P. Wrobel, K. Malek, S. Chlopicki, L. Mateuszuk, M. Baranska, *Analyst*, 2011, **136**, 5247
- 4 T.P. Wrobel, K. M. Marzec, K. Majzner, K. Kochan, M. Bartus, S. Chlopicki, M. Baranska, *Analyst*, 2012, **137**, 4135
- 5 K. Majzner, T. P. Wrobel, A. Fedorowicz, S. Chlopicki, M. Baranska, *Analyst*, 2013, **138**, 7400
- 6 J. Ollesch, S.L. Drees, H.M. Heise, T. Behrens, T. Brüning, K. Gerwert, *Analyst*, 2013, **138**, 4092
- 7 E. Staniszewska, A.K. Bartosz, K. Malek, M. Baranska, *Biomedical Spectroscopy and Imaging* 2013, **2**, 317
- 8 D. Perez-Guaita, J. Ventura-Gayete, C. Perez-Rambla, M. Sancho-Andreu, S. Garrigues, M. de la Guardia, *Microchem. J.*, 2013, **106**, 202
- 9 T. Vahlsing, U. Damm, V.R. Kondepoti, S. Leonhardt, M.D. Brendel, B.R. Wood, H.M. Heise, *J. Biophotonics*, 2010, **3**, 567
- 10 J. Ollesch, M. Heinze, H.M. Heise, T. Behrens, T. Brüning, K. Gerwert, *J. Biophotonics*, 2014, **7**, 210
- 11 K. Gajjar, J. Trevisan, G. Owens, P.J. Keating, N.J. Wood, H.F. Stringfellow, P.L. Martin-Hirsch, F.L. Martin, *Analyst*, 2013, **138**, 3917
- 12 J. Filik, M.D. Frogley, J.K. Pijanka, K. Wehbe, G. Cinque, *Analyst*, 2012, **137**, 853
- 13 P. Bassan, J. Lee, A. Sachdeva, J. Pissardini, K. M. Dorling, J. S. Fletcher, A. Henderson, P. Gardner *Analyst*, 2013, **138**, 144
- 14 K. Wehbe, J. Filik, M.D. Frogley, G. Cinque, *Anal Bioanal Chem*, 2013, **405**, 1311
- 15 T.P. Wrobel, B. Wajnchold, H.J. Byrne, M. Baranska, *Vib. Spectrosc.*, 2014, **71**, 115
- 16 P. Lasch, [www.cytospec.com](http://www.cytospec.com)
- 17 J. Filik, N. Stone, *Anal Chim Acta*, 2008, **616**, 177
- 18 F. Bonnier; F. Petitjean, M.J. Baker, H.J. Byrne, *J. Biophotonics*, 2014, **7**, 167
- 19 C. Ortiz, D. Zhang, Y. Xie, A.E. Ribbe, D. Ben-Amotz, *Anal. Biochem.*, 2006, **353**, 157
- 20 M. Romeo, M. Diem, *Vib. Spectrosc.*, 2005, **38**, 129
- 21 S. Kidoaki, T. Matsuda, *Langmuir*, 1999, **15**, 7639
- 22 V. Kopecký Jr., V. Baumruk, *Vib. Spectrosc.*, 2006, **42**, 184
- 23 C. Hughes, M. Brown, G. Clemens, A. Henderson, G. Monjardez, N.W. Clarke, P. Gardner, *J. Biophotonics*, 2014 DOI: 10.1002/jbio.201300167
- 24 Paul Bassan, Ashwin Sachdeva, Joe Lee, Peter Gardner, *Analyst*, 2013, **138**, 4139
- 25 S. Mitlin, K.T. Leung, *J. Phys. Chem. B*, 2002, **106**, 6234